2012

Computational Fluid Dynamics in Congenital Heart Disease

William M. DeCampli
Arnold Palmer Hospital for Children

I. Ricardo Argueta-Morales
Arnold Palmer Hospital for Children

Eduardo Divo
Embry-Riddle Aeronautical University, Eduardo.divo@erau.edu

Alain J. Kassab
University of Central Florida

Cardiology in the Young (2012), **22**, 800–808
doi:10.1017/S1047951112002028

Original Article

Computational fluid dynamics in congenital heart disease*

William M. DeCampli,[1,2] I. Ricardo Argueta-Morales,[1] Eduardo Divo,[3] Alain J. Kassab[4]

[1]Department of Cardiothoracic Surgery, The Heart Center, Arnold Palmer Hospital for Children; [2]Department of Medical Education, College of Medicine, University of Central Florida; [3]School of Engineering Technology, Daytona State College, Daytona Beach; [4]College of Engineering and Computer Science, Mechanical, Materials and Aerospace Engineering, University of Central Florida, Orlando, Florida, United States of America

Abstract Computational fluid dynamics has been applied to the design, refinement, and assessment of surgical procedures and medical devices. This tool calculates flow patterns and pressure changes within a virtual model of the cardiovascular system. In the field of paediatric cardiac surgery, computational fluid dynamics is being used to elucidate the optimal approach to staged reconstruction of specific defects and study the haemodynamics of the resulting anatomical configurations after reconstructive or palliative surgery. In this paper, we review the techniques and principal findings of computational fluid dynamics studies as applied to a few representative forms of congenital heart disease.

Keywords: Computational fluid dynamics; congenital heart disease; review

COMPUTATIONAL FLUID DYNAMICS IS A TECHNIQUE of determining fluid flow by numerically solving its equations of motion. Computational fluid dynamics has been a critical and invaluable tool in discovery, prediction, and validation of a wide variety of natural and artificial phenomena. In cardiovascular disease, computational fluid dynamics has been used to understand the contribution of flow disturbances to the evolution of atherosclerosis and risk factors for growth and rupture of aneurysms. Computational fluid dynamics is a crucial tool in the design of synthetic heart valves, stents, and ventricular assist devices. Given its broad applicability, it is not surprising that computational fluid dynamics should be a useful adjunct to our understanding and management of congenital heart disease. In this paper, we review the techniques and principal findings of computational fluid dynamics studies as applied to a few representative forms of congenital heart disease.

What is computational fluid dynamics?

Computational fluid dynamics is a technique that determines the behaviour of fluid flow using the laws of physics. In haemodynamics, these laws are the law of conservation of mass, conservation of linear momentum, embodied in Newton's laws of motion, and the laws of thermodynamics. The relevant physical properties of the materials under consideration – for example, density and viscosity – must also be known. In spite of this apparent complexity, the calculation of blood flow in biological systems is relatively straightforward, avoiding many of the features of more complicated fluid flow phenomena. The laws in differential form are expressed by the Navier–Stokes equations, as follows:

$$\nabla \cdot \vec{V} = 0 \; \textit{and} \; \rho \frac{\partial \vec{V}}{\partial t} + \rho(\vec{V} \cdot \nabla)\vec{V} = -\nabla p + \nabla \cdot \tau$$

where ρ denotes the fluid density, μ denotes the fluid viscosity, τ denotes the viscous stress tensor, p is the pressure, and $\vec{V}$ denotes the velocity vector.

*Presented in part at Cardiology 2012, 16th Annual Update on Pediatric and Congenital Cardiovascular Disease. Orlando, Florida, United States of America, February, 2012.

Correspondence to: Dr William M. DeCampli, MD, PhD, Department of Cardiothoracic Surgery, The Heart Center, Arnold Palmer Hospital for Children, 92 West Miller Street, Orlando, Florida 32806, United States of America. Tel: 321 843 3294; Fax: 321 841 4260; E-mail: william.decampli@orlandohealth.com

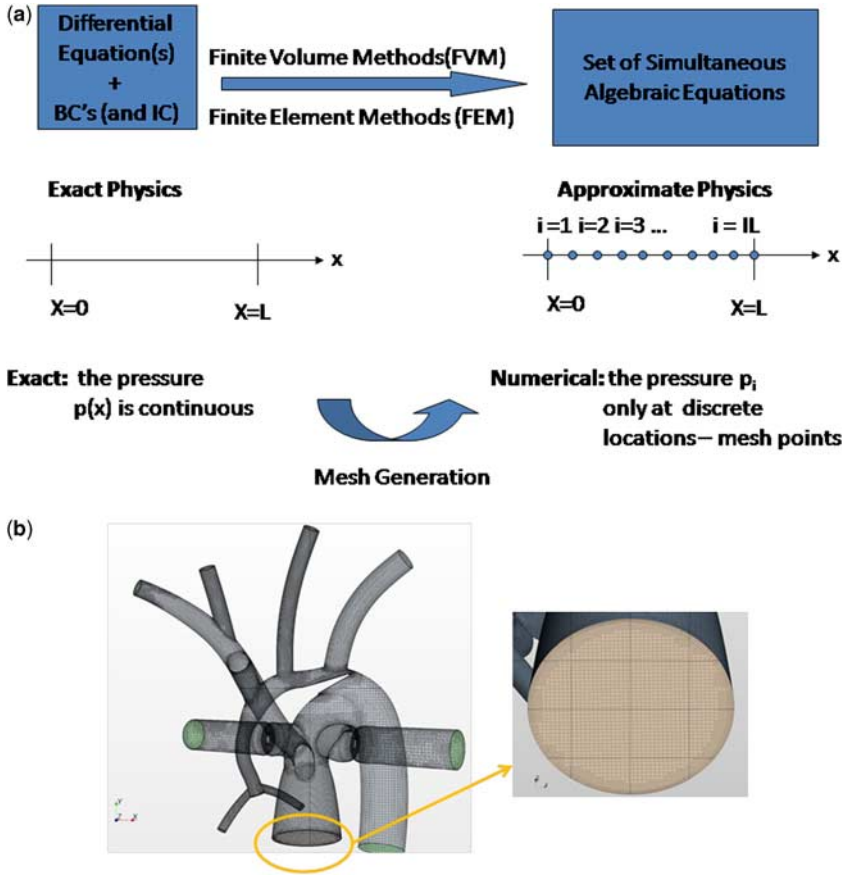

Figure 1.
*(**a**) Numerical methods generate an algebraic analogue to the continuous problem, (**b**) Example of a finite volume method mesh used for an analysis of the hybrid Norwood operation.[1] Here nearly 1.2 million cells are used to discretise the three-dimensional volume of interest for the haemodynamics analysis. (left) Hybrid Norwood topology with distal arch obstruction, (right) close-up of pulmonary root mesh. BC = boundary conditions; FEM = finite element methods; FVM = finite volume methods; IC = initial conditions.*

Although these equations are non-linear and generally cannot be solved analytically, they can always be solved using numerical techniques. Such techniques, most commonly finite volume or finite element methods, form the basis of computational fluid dynamics and use the fact that all differentials or integrals can be computed by approximating infinitesimally small changes (dx) as small but finite changes (Δx). A differential, or an integral, however complicated, is reduced to an analogous algebraic expression. Utilising this principle along with an appropriate accompanying representation of the continuum of interest by a distributed set of mesh points, or finite elements, produced by the process of mesh generation, an algebraic – discrete – analogue to the continuous problem is obtained over each gird volume or finite element, see Figure 1.[1] The resulting set of non-linear algebraic equations, which can number in the millions of equations, can be solved iteratively using computer workstations or clusters of workstations. Typically, resolving a time-accurate solution can take upwards of 2 or more days of computations.

Solving the equations of fluid flow requires that certain initial conditions and fixed conditions must be specified *a priori*. Examples include the resistances of vascular beds, parameters of the cardiac elastance function, and geometry – vessel size, shape, branching pattern, etc. – of the region of interest. In addition, *a priori* boundary conditions must be satisfied. Boundary conditions are imposed values of the calculated quantities – for example, velocity and pressure – at certain locations and times. For example, the velocity of flow at the inner surface of a blood vessel must be zero. Boundary conditions may be imposed by use of experimental or clinical information, such as catheter or magnetic resonance imaging data. In general, magnetic resonance data provide excellent velocity and flow, but not pressure data. Invasive catheterisation can provide some pressure information but at poor special resolution. In this sense, computational fluid

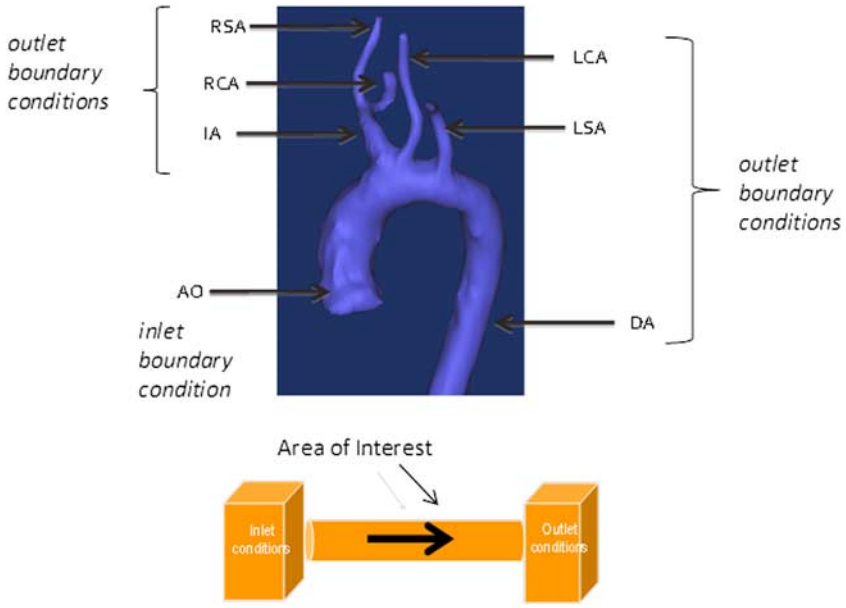

Figure 2.
Inlet (aortic root) and outlet (great vessels) boundary conditions for the aortic arch. AO = aorta; DA = descending aorta; IA = innominate artery; LCA = left carotid artery; LSA = left subclavian arteries; RCA = right carotid artery; RSA = right subclavian artery.

dynamics is not always a purely theoretical but may be a semi-empirical method that can calculate accurate pressure information at high resolution. Boundary conditions are satisfied by adjusting the solution in an iterative manner until the conditions are met. Sometimes, the boundary conditions themselves must be calculated from systems, often on a different scale, to which they are coupled. For example, we may be interested in the detailed flow characteristics in the aortic arch, using computational fluid dynamics. The "inlet" and "outlet" boundary conditions will be the flows and pressures at the aortic root, arch great vessels, and the distal arch (Fig 2).

These boundary flows and pressures, however, depend on cardiac function, and on the characteristics of all peripheral arterial beds, and hence must also be solved for. We refer to such problems as "multi-scale" problems. Computational fluid dynamics may not be required to compute the solution at the other scale, as parameterised – "lumped parameter" – models may suffice and save considerable computational time without loss of accuracy and physical meaning. A representative multi-scale design for analysing the Norwood circulation is shown in Figure 3.[1] In general, the extent to which a multi-scale solution is required depends on what one is attempting to demonstrate in the "region of interest".

Computational fluid dynamics is not a technique of *simulation* – it is a technique of *calculation*. In simulation, the behaviour of the phenomenon is generally already known. The objective of simulation is to reproduce the behaviour as realistically as possible, for application to training or to product testing. In computational fluid dynamics, the answer is not known ahead of time, and the method hence *discovers* the behaviour of fluid phenomena. The accuracy of the calculation is as good as that of the input initial and boundary conditions, and the precision is as good as the "fineness" of the finite volumes, or finite elements, and the theoretical power of the numerical technique used. The current capability of parallel processing allows very precise solution to the three-dimensional Navier–Stokes equations in non-steady haemodynamic flows within reasonable computational time. Typically not included in computational fluid dynamics calculations are biological effects such as auto-regulation, healing, and growth. Moreover, in most reported analysis the detailed compliance of the vessel walls is not taken into account, although there is a trend to include such a phenomenon through fluid-structure interaction modelling,[2,3] although models are still limited by the availability of constitutive models for the arterial wall.[4]

What can computational fluid dynamics tell us?

One's ability to intuit fluid flow is limited by the non-linear nature of the behaviour itself while computational fluid dynamics is able to provide such detailed solutions of the behaviour of fluid flow. From the computational solution, a myriad of phenomena can be described (Table 1). Many of

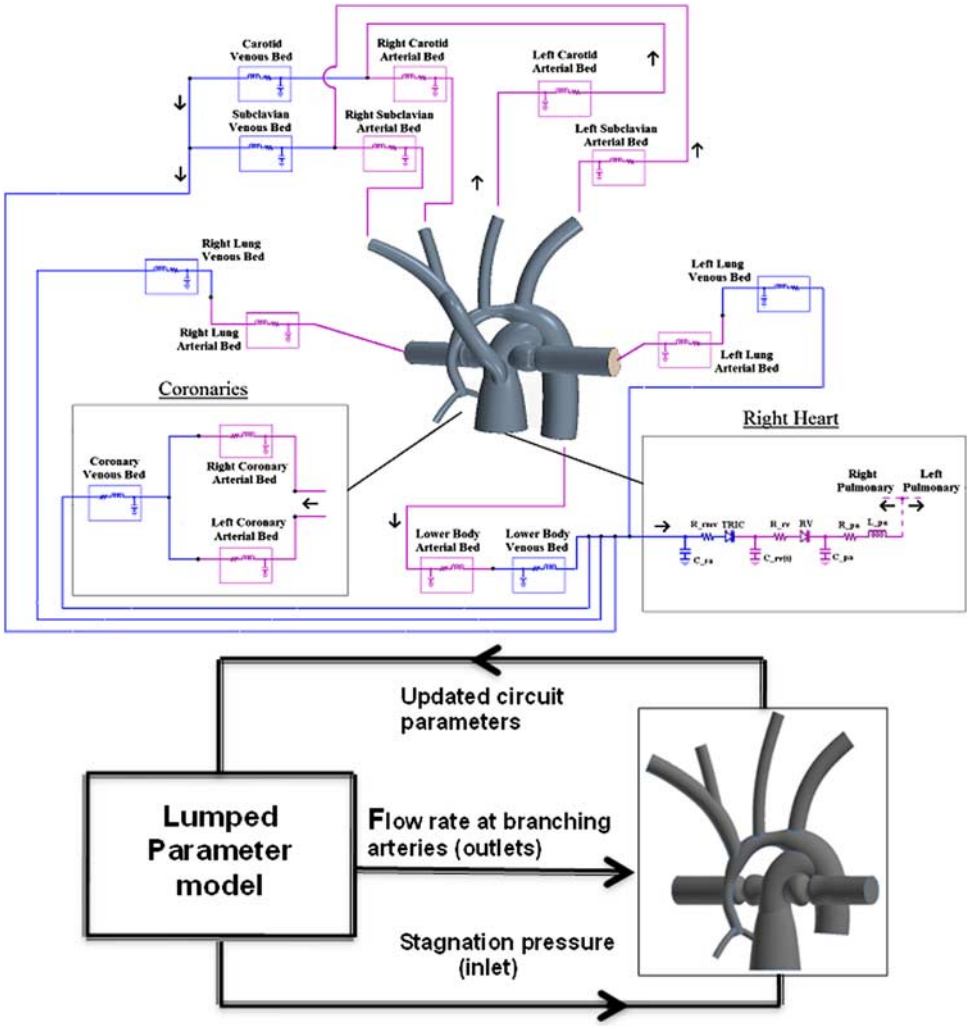

Figure 3.
Multi-scale design for analysing the hybrid Norwood circulation.

Table 1. Examples of flow phenomena that can be characterised by CFD.

Local pressures and flows
Flow distributions
Flow energy loss
Abnormal flow patterns, for example competitive flow, re-circulating flows, stagnation flow, etc.
Wall shear stress and normal stress
Oscillatory shear index
Shear stress gradient
Impact of vessel wall compliance
Impact on cardiac function

CFD = computational fluid dynamics

these phenomena have been linked empirically to pathological changes in cardiovascular structure and function. Thus, not only may computational fluid dynamics lead to the pathophysiology and mechanism of disease, but it may also lead to preventative or therapeutic measures to circumvent the disease.

Superior and total cavopulmonary connections

Some of the earliest work using computational fluid dynamics in congenital heart disease was applied to solving the optimal anatomic configuration of the superior cavopulmonary connection. As the pulmonary flow in such physiology is passive, it was believed that minimisation of flow energy loss, as well as the equal balance of flows to the left and right lungs, was at least theoretically related to clinical functional capacity and perhaps longevity. In these analyses, the usual endpoints of the calculation were (1) the ratio of left pulmonary artery and right pulmonary artery flow rate and (2) the fraction of incoming hydraulic power dissipated, with the hydraulic power being defined as

$$W = \left(\frac{1}{2}\rho V^2 + p\right)Q$$

where ρ is the density of blood and V, p, and Q are the mean velocity, pressure, and flow rate, respectively, at

each inlet and outlet of the region of interest – specifically, the caval vein, hepatic veins, and branch pulmonary arteries at the lung hila. The fractional power dissipated was defined as $(W_{inlet} - W_{outlet})/W_{inlet}$. This value is in the range of 1 mW in a typical Fontan configuration. The optimal surgical configuration was defined as that which rendered the minimum fractional power dissipation and the best balance of left and right lung flows. In the earliest work,[5] it was predicted that the optimal configuration was that of the inferior cavopulmonary connection "extended" towards the right pulmonary artery relative to the superior caval connection. These early predictions were limited by *a priori* knowledge of input boundary conditions – from limited magnetic resonance velocity data – as well as the lack of consideration of vessel elasticity and the effects of ventilation. Over the next 15 years, considerable improvements were made in these calculations owing to (1) better resolution of magnetic resonance imaging, (2) improved computing power, and (3) the use of real patient data to configure the anatomy. Hsia et al[6] recalculated the cavopulmonary optimisation scheme, comparing the lateral tunnel, intra-atrial tube, and extracardiac conduit – offset to the left or to the right of the superior caval anastomosis. They found the optimal configuration to be that of a 19–20-mm extracardiac conduit offset to the left of the superior caval vein. Much smaller, and much larger diameter conduits had greater power loss. The range in fractional power loss was not very large: 0.081 for the optimal configuration and 0.11 for the conduit offset to the right of the superior caval vein, and the range in left to right lung flow ratio was 0.9 to 1.1. Socci et al[7] and Sundareswaran et al[8] confirmed many of the flow characteristics in further analyses.

Marsden et al[9] investigated the fluid dynamics of a Y-graft configuration for the inferior cavopulmonary connection in a patient-specific model using magnetic resonance data and computational fluid dynamics. Their study included a model for ventilator effect and for exercise, the latter being modelled simply as an increase in input flow rate. Compared with standard single extracardiac conduits – with and without offset – the Y-graft with 12-mm-diameter branches had (1) lower fractional power dissipation during rest and exercise, (2) lower superior caval vein pressure during exercise, (3) greater equilibration of left and right lung flow, and (4) larger regions of low shear stress.

Whitehead et al[10] further investigated power dissipation during modelled exercise. They used resting magnetic resonance data from 10 patients and thus generated 10 baseline models to investigate. They determined the presence of a non-linear relation between flow rate – the exercise parameter – and power dissipation. An exercise level of three times baseline flow resulted in power dissipation equivalent to nearly *doubling* the pulmonary vascular resistance. They argued that this effect could substantially increase "Fontan pressures", as well as limit effective cardiac output. They also found that pulmonary flow splits substantially affected power dissipation.

Itatani et al[11] investigated the effect of conduit diameter on power dissipation and on the volume of flow stagnation, that is, regions of flow velocity <1 cm/s. They used velocity and flow data from 17 Fontan patients to form input boundary conditions and to design the representative anatomy. These data included clinical magnetic resonance velocities both a rest and two levels of exercise. They also modelled ventilation. Using computational fluid dynamics, they found resting power dissipation of 1.5–1.7 mW, or 6–7% of input power. At 1 W/kg exercise, power dissipation was 4–6 mW, or 9.6–12.5% of input power. The dependence on conduit sizes, ranging from 14 to 22 mm, was monotonic and most pronounced during 1 W/kg exercise – the larger the conduit, the less the power dissipation. Larger conduits, however, were associated with greater stagnation volume. The greatest stagnation volumes occurred at rest, in the expiratory ventilator phase, and in the larger – 20–22 mm– conduits. The value reached 5.2 ml, or 34% of the 22-mm conduit volume. The authors suggested the optimal conduit size to be in the 18–19-mm range.

Norwood procedure and variants

Computational fluid dynamics studies of the Norwood circulation began with an analysis, by Migliavacca et al,[12] of flow in a systemic to pulmonary artery shunt. They investigated the shunt pressure drop–flow relationship, varying shunt implantation angle, diameter, curvature, and input pulsatility and found, as expected, that shunt diameter was the main determinant of graft flow. Most of the pressure drop occurred near the proximal anastomosis, and curved grafts resulted in a lower pressure drop as compared with straight grafts, owing to reduced flow-line skewness towards the lateral graft wall near the proximal anastomosis. They found that inertial effects – pulsatility – had little influence on the solutions. In a follow-up study,[13] they investigated the Norwood circulation using a three-compartment "lumped-parameter" model, using available clinical data to derive input and boundary conditions. The compartments included the heart model, and systemic and pulmonary circulations. They varied shunt sizes from 3–5 mm and determined that larger shunt diameters

diverted cardiac output to the lungs, thereby diminishing O_2 delivery and that maintaining a pulmonary to systemic blood flow ratio of 1 provided optimal O_2 delivery across investigated heart rate and shunt size combinations. From the computational fluid dynamics solutions, they derived expressions that allowed clinical estimation of shunt flow from Doppler-derived pressure drop data.[14]

Multi-scale computational fluid dynamics analysis of the variants of the Norwood reconstructive surgeries were compared with post-operative catheterisation and Doppler data.[15,16] In these studies, the Norwood operation with a modified Blalock–Taussig shunt was compared with the right ventricle-to-pulmonary artery shunt modification. They found good correlation between computational fluid dynamics solutions and observed post-operative clinical data, further buttressing confidence in the predictive capabilities of the multi-scale computational fluid dynamics analysis as an effective tool for pre-operative planning. The model predicted that the right ventricle shunt would result in higher aortic diastolic pressure, decreased pulmonary arterial pressure, lower pulmonary to systemic flow, and higher coronary perfusion relative to the innominate artery-to-right pulmonary artery shunt. Moreover, examination of detailed flow profiles in the right ventricle-to-pulmonary artery shunt led the authors to predict minimal regurgitation through the conduit, which was consistent with clinical measurements. The size of the shunt is critical for the innominate artery-to-right pulmonary artery operation as the larger shunts lead to detrimental haemodynamics, although larger shunts are needed for the right ventricle shunt to achieve satisfactory arterial oxygenation. The authors report a non-intuitive result predicted by the model, namely, that the afterload in the right ventricle-to-pulmonary artery configuration is lower than that of the innominate artery-to-right pulmonary artery configuration because of flow through the right ventricle shunt before the aortic valve opening, resulting in reduced ventricular wall shear stress at equal pressure. In a follow-up study, Hsia et al[17] utilised multi-scale analysis in a surgical planning setting to compare alternatives to management of stenotic right ventricle-to-pulmonary artery shunt after the Norwood procedure, namely: (1) conversion to a modified Blalock–Taussig shunt and (2) augmenting the existing right ventricle-to-pulmonary artery shunt with an additional modified Blalock–Taussig shunt. They concluded that the second option can lead to pulmonary overcirculation and recommended that the stenotic shunt be taken down and conversion to an optimal modified Blalock–Taussig shunt be undertaken.

Multi-scale computational fluid dynamics analysis has been applied to study another variant, the so-called hybrid Norwood approach. A multi-scale computational fluid dynamics analysis was used by Corsini et al[18] to examine the role of the stented arterial duct and the degree of pulmonary banding to achieve the balance of Q_p/Q_s, cardiac output, and O_2 delivery to optimize patient survival in the hybrid Norwood. They concluded that oxygen delivery was most sensitive to the degree of branch pulmonary banding rather than to the ductal stent size. Ceballos et al[1,19] utilised a multi-scale analysis of the hybrid Norwood operation using a synthetic but anatomically appropriate reconstruction of the vasculature and considered the effect of distal arch obstruction on the hybrid Norwood circulation with and without the presence of a reverse

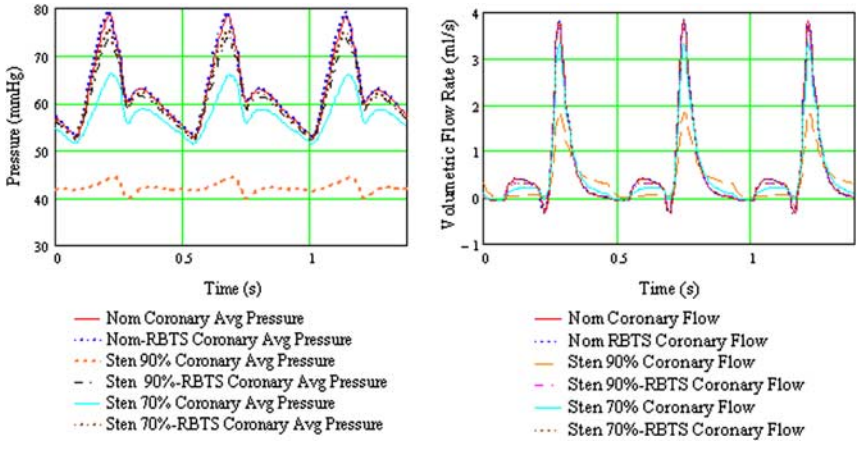

Figure 4.
Composite plot of average coronary pressure and flow for the six configurations considered for the hybrid Norwood analysis. mmHg = millimetres of mercury; Nom = nominal (baseline model, no aortic arch stenosis); RBTS = reverse Blalock–Taussig shunt; s = seconds; Sten 90 = model with 90% distal aortic arch obstruction; Sten 70% = model with 70% distal arch obstruction.

Table 2. Results from multi-scale CFD analysis of six configurations considered in the hybrid Norwood operation – Cardiac output, arterial flow rates, and flow changes for all anatomical configurations.

Model	Cardiac output (ml/min)	Qp/Qs	Flow rate as percentage of cardiac output									
			DA	LCA	LcorA	LPA	LSA	RCA	RcorA	RPA	RSA	Shunt
Nominal	2015	0.94	29.4	4.6	1.8	24.1	4.7	4.6	1.8	24.3	4.7	
Nominal-RBTS	2022	0.93	29.4	4.7	1.8	24.0	4.7	4.6	1.8	24.3	4.7	11.7
Stenosis 90%	1863	1.10	31.9	3.2	1.3	26.1	3.3	3.2	1.3	26.3	3.2	
Stenosis 90%-RBTS	1975	0.94	29.7	4.5	1.8	24.1	4.6	4.6	1.8	24.3	4.6	21.3
Stenosis 70%	1926	0.95	29.9	4.4	1.8	24.3	4.5	4.4	1.8	24.5	4.4	
Stenosis 90%-RBTS	1990	0.94	29.7	4.6	1.8	24.1	4.6	4.6	1.8	24.3	4.6	14.3
	Percentage of flow change from Nominal											
Nominal-RBTS	0.35	−0.2	0.3	0.5	0.3	0.3	0.5	0.7	0.3	0.3	0.7	
Stenosis 90%	−7.54	17.8	0.4	−35.7	−31.7	0.3	−35.7	−35.7	−31.7	0.3	−35.7	
Stenosis 90%-RBTS	−1.99	0.3	−1.0	−4.3	−2.1	−1.8	−4.4	−3.7	−2.0	−1.8	−3.7	
Stenosis 70%	−4.42	2.0	−2.8	−9.2	−5.3	−3.4	−9.3	−9.2	−5.3	−3.5	−9.3	
Stenosis 90%-RBTS	−1.24	0.1	−0.4	−3.0	−1.3	−1.2	−3.0	−2.5	−1.3	−1.2	−2.5	

DA = descending aorta; LCA = left carotid artery; LcorA = left coronary artery; LPA = left pulmonary artery; LSA = left subclavian artery; Qp/Qs = pulmonary to systemic flow ratio; RBTS = reverse Blalock–Taussig shunt; RCA = right carotid artery; RcorA = right coronary artery; RPA = right pulmonary artery; RSA = right subclavian artery

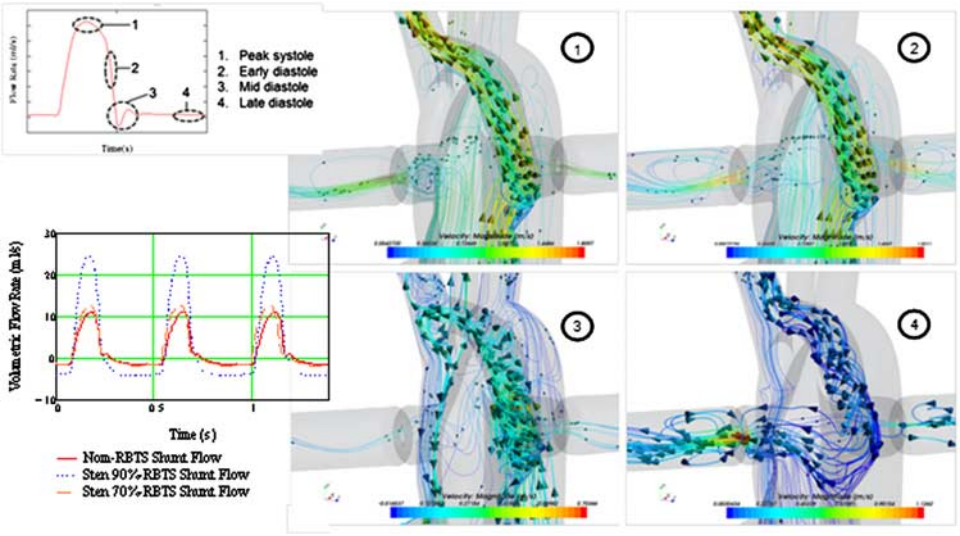

Figure 5.
Close-up examination of the reverse Blalock–Taussig shunt graft flow when the shunt is placed "preventatively", that is, before significant distal arch obstruction develops. Detailed pathlines exhibit swirling flow with several zones of recirculation and low velocity for a good fraction of the cardiac cycle. Nom = nominal (baseline model, no aortic arch stenosis); RBTS = reverse Blalock-Taussig shunt; Sten 90% = model with 90% distal aortic arch obstruction; Sten 70% = model with 70% distal arch obstruction.

Blalock–Taussig shunt from the pulmonary root to the innominate artery.

The analysis showed that a 90% distal arch stenosis reduced pressure and net flow rate through the coronary and carotid arteries by 30% (Table 2 and Fig 4). Addition of a 4-mm × 21-mm reverse Blalock–Taussig shunt completely restored pressure and flow rate to baseline in these vessels. Zones of flow stagnation, flow reversal, and recirculation in the presence of stenosis were rendered more orderly by addition of the reverse Blalock–Taussig shunt. In the absence of stenosis, a "preventatively" placed shunt resulted in extensive zones of disturbed flow within the reverse Blalock–Taussig shunt consisting of zones with thrombogenic potential (recirculation and stagnation that persist for a substantial fraction of the cardiac cycle) (Fig 5; see Supplementary Material, Videos 1 and 2).

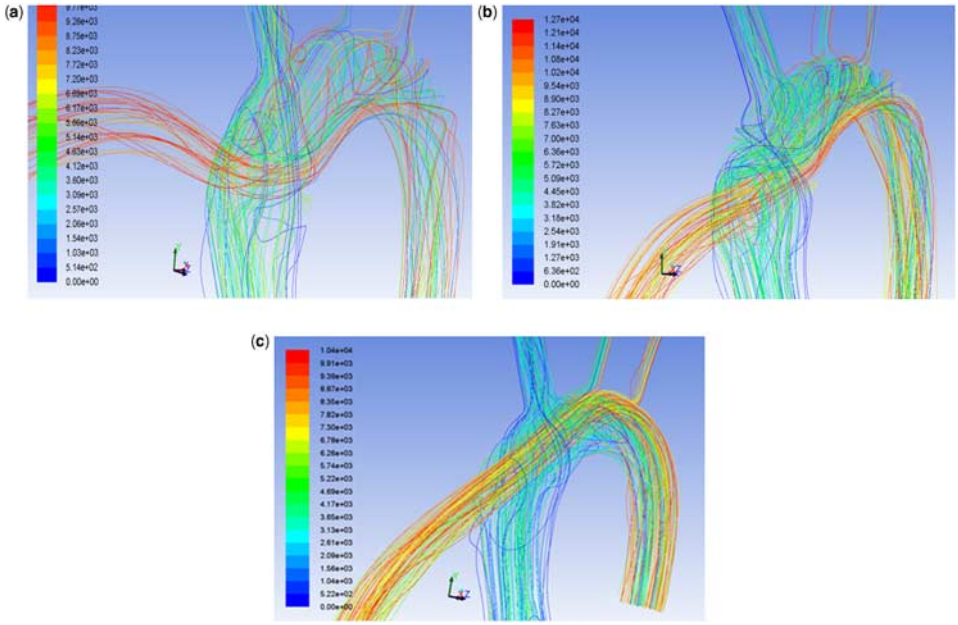

Figure 6.
The Infant model flow pathlines for perpendicular (left), intermediate (middle), and shallow (right) ventricular assist device outflow graft anastomotic angles. These three models resulted in significantly different probabilities of cerebral thromboembolism from thrombi originating proximal to the distal end of the assist device outflow graft.

Optimisation of left ventricular assist device implantation to reduce stroke risk

Using computational fluid dynamics studies, Osorio et al[20] and Argueta-Morales et al[21] reported as much as a 50% reduction of cerebral thromboembolism by tailoring of the angle and placement of the of ventricular assist device outflow cannula in adult computer-generated and patient-specific calculations. The flow field was resolved in the steady state, representative of low pulsatility conditions of continuous-flow assist devices, and thrombus paths were computed using a Lagrangian model. The trajectories of smaller size particles – (thrombi) with low momentum essentially followed the streamlines, whereas those of larger particles with higher momentum deviated from the streamlines (see Supplementary Material, Videos 3 and 4). Computations to study blood flow patterns and particle tracks originating in the assist device were carried out on representative three-dimensional aortic arch models for Infant (4 kg) and Child (20 kg) models.[22] The percentage of particles entering cerebral vessels was calculated for 14 implantation configurations for an 8-mm assist device outflow graft. Figure 6 shows flow pathlines for three different implantation angles. For both models, the percentage of particles entering the cerebral vessels varied by as much as 50% depending on the implantation configuration. In the Infant model, there is a "smoother" transition of flow into the aortic arch because the assist device outflow graft diameter is equal to the ascending aorta. Decreasing the anastomosis angle directs the blood flow straight into the cerebral vessels, resulting in an increased risk of embolisation. In the Child model, shallower angle and more cephalad placement of the assist device outflow graft anastomosis prevents formation of recirculation zones in the ascending aorta, decreasing the cerebral embolisation rate (see Supplementary Material, Videos 5 and 6).

Conclusions

Computational fluid dynamics is a numerical technique that determines the behaviour of fluid flow using the laws of physics. When coupled with a multi-scale approach to impose the inlet and outlet boundary conditions of an isolated portion of the vasculature, computational fluid dynamics augments clinical data obtained by standard imaging and interventional techniques. The technique has a wide range of applications, including those reviewed herein, as well many others such as aortic coarctation[23] and Kawasaki disease.[24] It may aid in improving our understanding of the pathophysiology and mechanism of cardiovascular disease, in elucidating measures to treat these diseases, and in surgical planning.[25]

Supplementary Materials

For the supplementary materials referred to in this article, please visit http://dx.doi.org/doi:10.1017/S1047951112002028

References

1. Ceballos A, Argueta-Morales IR, Divo EA, et al. Computational analysis of hybrid Norwood circulation with distal aortic arch obstruction and reverse Blalock–Taussig shunt. Ann Thorac Surg, 2012; 94: 1540–1550.
2. Long CC, Hsu MC, Bazilevs S, Feinstein JA, Marsden AL. Fluid–structure interaction simulations of the Fontan procedure using variable wall properties. Int J Numer Meth Biomed Engng 2012; 28: 513–527.
3. Humphrey JD, Holzapfel GA. Mechanics, mechanobiology, and modeling of human abdominal aorta and aneurysms. J Biomech 2012; 45: 805–814.
4. Gasser TC, Ogden RW, Holzapfel GA. Hyperelastic modelling of arterial layers with distributed collagen fibre orientations. J R Soc Interface 2006; 3: 15–35.
5. de Leval MR, Dubini G, Migliavacca F, et al. Use of computational fluid dynamics in the design of surgical procedures: application to the study of competitive flows in cavo-pulmonary connections. J Thorac Cardiovasc Surg 1996; 111: 502–513.
6. Hsia TY, Migliavacca F, Pittaccio S, et al. Computational fluid dynamic study of flow optimization in realistic models of the total cavopulmonary connections. J Surg Res 2004; 116: 305–313.
7. Socci L, Gervaso F, Migliavacca F, et al. Computational fluid dynamics in a model of the total cavopulmonary connection reconstructed using magnetic resonance images. Cardiol Young 2005; 15 (Suppl 3): 61–67.
8. Sundareswaran KS, Pekkan K, Dasi LP, et al. The total cavopulmonary connection resistance: a significant impact on single ventricle hemodynamics at rest and exercise. Am J Physiol Heart Circ Physiol 2008; 295: H2427–H2435.
9. Marsden AL, Bernstein AJ, Reddy VM, et al. Evaluation of a novel Y-shaped extracardiac Fontan baffle using computational fluid dynamics. J Thorac Cardiovasc Surg 2009; 137: 394–403.
10. Whitehead K, Pekkan K, Kitajima HD, Paridon SM, Yoganathan AP, Fogel MA. Nonlinear power loss during exercise in single-ventricle patients after the Fontan. Circulation 2007; 116 (Suppl I): I165–I171.
11. Itatani K, Miyaji K, Tomoyasu T, et al. Optimal conduit size of the extracardiac Fontan operation based on energy loss and flow stagnation. Ann Thorac Surg 2009; 88: 565–572.
12. Migliavacca F, Dubini G, Pennati G, et al. Computational model of the fluid dynamics in systemic-to-pulmonary shunts. J Biomech 2000; 33: 549–557.
13. Migliavacca F, Pennati G, Dubini G, et al. Modeling of the Norwood circulation: effects of shunt size, vascular resistances, and heart rate. Am J Physiol Heart Circ Physiol 2001; 280: H2076–H2086.
14. Migliavacca F, Yates R, Pennati G, Dubini G, Fumero R, de Leval MR. Calculating blood flow from Doppler measurements in the systemic-to-pulmonary artery shunt after the Norwood operation: a method based on computational fluid dynamics. Ultrasound Med Biol 2000; 26: 209–219.
15. Migliavacca F, Balossino R, Pennati G, et al. Multiscale modelling in biofluidynamics: application to reconstructive paediatric cardiac surgery. J Biomech 2006; 39: 1010–1020.
16. Bove EL, Migliavacca F, de Leval MR, et al. Use of mathematic modeling to compare and predict hemodynamic effects of the modified Blalock–Taussig and right ventricle-pulmonary artery shunts for hypoplastic left heart syndrome. J Thorac Cardiovasc Surg 2008; 136: 312–320.
17. Hsia TY, Migliavacca F, Pennati G, et al. Management of a stenotic right ventricle-pulmonary artery shunt early after the Norwood procedure. Ann Thorac Surg 2009; 88: 830–837.
18. Corsini C, Cosentino D, Pennati G, Dubini G, Hsia TY, Migliavacca F. Multiscale models of the hybrid palliation for hypoplastic left heart syndrome. J Biomech 2011; 44: 767–770.
19. Ceballos A, Kassab A, Osorio R, et al. A multiscale model of the neonatal circulatory system following hybrid Norwood palliation. Abstract 172, Society of Thoracic Surgeons (STS) 48th Annual Meeting, Fort Lauderdale, Florida, January 30–February 1, 2012.
20. Osorio AF, Osorio R, Ceballos A, et al. Computational fluid dynamics analysis of surgical adjustment of left ventricular assist device implantation to minimize stroke risk. Comput Methods Biomech Biomed Engin, 2011 [ahead of print]. http://dx.doi.org/10.1016/j.athoracsur.2012.06.043.
21. Argueta-Morales IR, Tran R, Clark W, Divo E, Kassab A, DeCampli WM. Use of Computational Fluid Dynamics (CFD) to tailor the surgical implantation of a Ventricular Assist Device (VAD): a patient-specific approach to reduce risk of stroke. J Am Coll Surg 2010; 211 (3 Suppl): 26–27.
22. DesJardins S, Argueta-Morales IR, Ceballos A, et al. Tailoring the surgical placement of pediatric Ventricular Assist Devices (VAD) may reduce stroke risk. World J Pediatr Congenit Heart Surg 2011; 2: 187.
23. Coogan JS, Chan FP, Taylor CA, Feinstein FA. Computational fluid dynamic simulations of aortic coarctation comparing the effects of surgical and stent-based treatments on aortic compliance and ventricular workload. Catheter Cardiovasc Interv 2011; 77: 680–691.
24. Sengupta D, Kahn AM, Burns JC, Sankaran S, Shadden S, Marsden A. Image-based modeling of hemodynamics and coronary artery aneurysms caused by Kawasaki disease. Biomech Model Mechanobiol 2012 [ahead of print]. doi 10.1007/s10237-011-0361-8.
25. Baretta A, Corsini C, Yang W, et al and The Modeling of Congenital Hearts Alliance (MOCHA) Investigators. Virtual surgeries in patients with congenital heart disease: a multi-scale modelling test case. Phil Trans R Soc A 2011; 369: 4316–4330.